

**RESEARCH ARTICLE** OPEN ACCESS

# Fundamental Studies on “Blue Titania” Under Oxygen-Free Conditions: Color Evolution and Stability as Function of the Crystal Phase

Felix Lorenz<sup>1</sup> | Nikolaos G. Moustakas<sup>1</sup> | Akbar Valaei<sup>2</sup> | Paul Kuschmitz<sup>3</sup> | Ian G. Shuttleworth<sup>4</sup> | Helge Stein<sup>5</sup>  | Tim Peppel<sup>1</sup>  | Dirk Ziegenbalg<sup>2</sup> | Jennifer Strunk<sup>1,6</sup> 

<sup>1</sup>Leibniz Institute for Catalysis, Rostock, Germany | <sup>2</sup>Ulm University, Institute of Chemical Engineering, Ulm, Germany | <sup>3</sup>German Aerospace Center, Institute for Frontier Materials on Earth and in Space, Aerogels and Highly Porous Materials, Köln, Germany | <sup>4</sup>Tapestry Learning Partnership, Sherwood Rise, Nottingham, UK | <sup>5</sup>Technical University of Munich, Chair for Digital Catalysis, Garching/München, Germany | <sup>6</sup>Technical University of Munich, Chair for Industrial Chemistry and Heterogeneous Catalysis, Garching/München, Germany

**Correspondence:** Jennifer Strunk ([jennifer.strunk@tum.de](mailto:jennifer.strunk@tum.de))

**Received:** 19 December 2025 | **Revised:** 13 May 2026 | **Accepted:** 22 May 2026

**Keywords:** aerogel | amorphous solid | anatase | charge carrier | chemical engineering | crystal | materials science | particle size | photocatalysis | rutile

## ABSTRACT

“Blue titania” is widely applied in photocatalysis, but comparative studies on the influence of the TiO<sub>2</sub> phase on color evolution and stability are rare. Here, this knowledge gap is closed by evaluating comparatively the formation of blue titania from pure anatase, pure rutile, P25 (~80% anatase, 20% rutile), and partially amorphous materials. The blue color is attained by photocatalytic reaction of 2-propanol on TiO<sub>2</sub> under oxygen-free conditions. It is additionally evaluated how different irradiation conditions and the intentional presence of oxygen influence TiO<sub>2</sub> coloration. A high surface area is found to lead to rapid discoloration. Rutile is more stable against discoloration in air than an anatase of similar particle size. The mixed-phase material P25 shows exceptional behavior: It reaches the strongest blue color and retains the color the longest time under ambient conditions. In the presence of oxygen, photooxidation of 2-propanol still causes a blue color of TiO<sub>2</sub>, which is explained by a slow transfer of photogenerated electrons over the interface. Insights gained with standard materials is complemented by experiments with an engineered aerogel material previously shown to be remarkably active in the storage of charge carriers. The influence of restricted oxygen diffusion in pressed aerogel pellets is also discussed.

## 1 | Introduction

Titanium dioxide in its native state is a white pigment, yet color changes upon reduction have been well known for more than a century. For instance, TiO<sub>1.50</sub> exhibits a dark violet, TiO<sub>1.60–1.73</sub> a blueish black, and TiO<sub>1.75–1.97</sub> a dark blue color, respectively [1–3]. Furthermore, Zeffoss et al. were the first to show that rutile single crystals undergo color changes in H<sub>2</sub> atmosphere at temperatures above 600°C from transparent greenish, into slightly blue, darker blue, and finally black. This behavior was determined to be completely reversible in O<sub>2</sub> atmosphere [4]. Johnson and Weyl thoroughly investigated the color and electrical properties of rutile

soon after. They concluded that the blue color change was caused, for example, by the incorporation of cations with higher valence (e.g., Sb<sup>V</sup>, Ta<sup>V</sup>, W<sup>VI</sup>, Mo<sup>VI</sup>) into the rutile lattice. It is assumed to be based on the formation of Ti<sup>3+</sup> ions, whose light absorption is increased as a result of strong deformation by the lattice forces [5]. The phototrophic behavior of rutile under UV irradiation was investigated in detail by Williamson. Photoreductive experiments and kinetic investigations were performed by Renz and Jacobsen, respectively [6, 7]. Weyl and Förland proposed a so-called “memory effect” of TiO<sub>2</sub>. They concluded from their experiments that the structure of TiO<sub>2</sub> remains intact while molecular oxygen is liberated under photoreduction [8]. Indeed, as

This is an open access article under the terms of the [Creative Commons Attribution](https://creativecommons.org/licenses/by/4.0/) License, which permits use, distribution and reproduction in any medium, provided the original work is properly cited.

© 2026 The Author(s). *ChemPhotoChem* published by Wiley-VCH GmbH.

discussed in detail by Diebold [9], when TiO<sub>2</sub> single crystals are heated in vacuum to very high temperatures, oxygen is removed from the lattice, i.e., the material is reduced thermally, and oxygen vacancy formation is associated with the formation of two Ti<sup>3+</sup> cations. Under extreme conditions, e.g., almost 5 h at 1450 K, the samples might appear virtually black [9].

Such black titania has been used in photocatalysis since the seminal work by Mao et al. in 2011, where it was found to be a highly active and stable visible light photocatalyst for hydrogen evolution from aqueous alcohol solutions [10]. The high stability of the material has been attributed to a strongly disordered shell around a crystalline TiO<sub>2</sub>. Here, however, the black TiO<sub>2</sub> powder has not been obtained by thermal reduction, but by treatment under 20 bar H<sub>2</sub> at 200°C for 5 days. It should also be noted that hydrogen evolution with blue titania had already been reported in 2010 [11]. Moreover, in both Mao's and Feng's work, apart from a sacrificial reagent, a Pt cocatalyst was used for hydrogen evolution.

Blue TiO<sub>2</sub> is not only studied in photocatalysis, but it has also been suggested as an anode material in batteries for fast lithium storage [12–14]. Today, a variety of methods have been suggested to obtain blue or black titania, ranging from classical treatments under hydrogen, high pressure, and temperature [10, 13], over chemical reductions with, e.g., NaBH<sub>4</sub> [15], alkaline metals [16] or metallic aluminum nanoparticles [14], to flame synthesis from TiCl<sub>4</sub> [17] and direct (combustion) synthesis methods from titanium alcoholate or halide precursors [11, 18, 19]. The large variety of synthesis methods and TiO<sub>2</sub> polymorphs studied makes it difficult to compare the influence of the reaction conditions and crystal phase on TiO<sub>2</sub> coloration systematically. While the blue or black color is traditionally attributed to oxygen deficiency, Ti<sup>3+</sup> cations, and possibly amorphous shells, it has also been proposed that highly crystalline blue TiO<sub>2</sub> may be obtained through hydrogenation upon reaction with TiH<sub>2</sub> [20]. So, the blue color may also be associated with Ti–H or Ti–OH groups, or a general upshift of the valence band edge [21]. For samples prepared by a solvent evaporation method, it has even been found that different material properties of black TiO<sub>2</sub> were obtained after calcination in Ar atmosphere compared to calcination in N<sub>2</sub>. It is, thus, expected that there is more than one chemical state of the TiO<sub>2</sub> that makes it appear blue or black.

Previous studies have shown that TiO<sub>2</sub> is capable of oxidizing 2-propanol in the presence of oxygen. In this process, the selective oxidation product acetone is found on the TiO<sub>2</sub> surface and in the gas phase. As reaction time progresses, increasing amounts of species with a carboxylate group, likely acetates, formed by subsequent reactions block the surface, so photocatalytic activity decreases, despite some of these side products eventually desorbing as CO<sub>2</sub> [22]. Related reactions have also been studied in detail on TiO<sub>2</sub> single crystal surfaces, where the decomposition of acetates was found to be 10 times slower than alcohol decomposition [23, 24]. In aerobic photocatalytic oxidation reactions of alcohols on titania, the oxidation of the alcohol with photogenerated holes is facile and quick, whereas the electron transfer for the activation of oxygen to superoxide progresses slowly on bare titania [25]. This is detectable by IR spectroscopy because the accumulation of excess electrons causes a tilting of the spectral baseline, starting at around ~2000 cm<sup>-1</sup> toward lower wavenumbers [25]. Electron transfer can be accelerated, for example, by depositing

gold nanoparticles on the surface of TiO<sub>2</sub>, which attract excess electrons and catalyze oxygen activation [26]. On the contrary, even in the absence of gold and oxygen, 2-propanol can still be oxidized to some extent, but since electrons can no longer be removed by superoxide formation, even more excess electrons remain inside of TiO<sub>2</sub>, leading to a more strongly tilted baseline in the IR spectra [25]. It is also visible to the naked eye, because TiO<sub>2</sub> will become intensely blue colored. In a related manner, Bahnemann et al. first proposed a connection between excess electrons and a broad absorption of TiO<sub>2</sub> around 650 nm [27]. In other words, the immediate oxidation of 2-propanol or other alcohols on TiO<sub>2</sub> by photogenerated holes, together with the slow reaction of electrons, can also be used to purposefully induce a net reduction of TiO<sub>2</sub> when no oxygen is present in the surrounding atmosphere. This can be considered as a storage of reduction equivalents in photocatalysts for later use, an approach also termed as “dark photocatalysis” [28]. Such an approach has also been used previously for TiO<sub>2</sub> aerogels in aqueous methanolic solution, where it was termed “photocharging” [29]. Compared to high-temperature and/or high-pressure treatments, the reduction with alcohols at room temperature is least likely to cause changes to the TiO<sub>2</sub> polymorph, such as the formation of amorphous shells, or potential rutilization at high temperature.

Here, using a high-purity gas-phase photoreactor that assures the absence of oxygen (<1 ppm), we aim to close the knowledge gap on the behavior of different TiO<sub>2</sub> phases in their blue state. All TiO<sub>2</sub> samples are identically reduced by functioning as an oxidant for 2-propanol in a gas-solid reaction without any solvent, to compare the achievable extent of reduction and the color. To link our observations to previous work, specialized aerogel materials previously used for hydrogen generation by “dark photocatalysis” are studied by a related procedure.

## 2 | Experimental

### 2.1 | Commercial Samples

Four different commercially available TiO<sub>2</sub> materials are used; pure anatase (*IoLiTec*, 10–30 nm), pure rutile (*IoLiTec*, 10–30 nm), P25 (Evonik Industries, ~80% anatase, ~20% rutile, as declared by the supplier), and Hombikat UV100 (anatase, <10 nm, surface area >250 m<sup>2</sup> g<sup>-1</sup>). To prepare the samples for the test in the photoreactor, 1 g of each TiO<sub>2</sub> was pressed into a pellet with a diameter of 30 mm, resulting in a thickness of approximately 1 mm. For some experiments, pellets were prepared consisting of more than one TiO<sub>2</sub> powder, as will be explained in detail with the presentation of the results.

### 2.2 | Synthesis of TiO<sub>2</sub> Aerogels

The synthesis of the aerogels has been reported previously in Ref. [29]. In brief, titanium(IV) isopropoxide (TTIP) was used as precursor in an acid-catalyzed sol–gel synthesis, with molar ratios of TTIP/ethanol/acid/water of 1:26:0.1:4. The obtained gels were aged at 50°C for 7 days, then washed four times with isopropanol, and finally dried with CO<sub>2</sub> at supercritical conditions. As reported in Ref. [29], the obtained aerogel is semi-crystalline,

consisting of an anatase phase and an amorphous phase. It exhibits a specific surface area of  $600 \text{ m}^2 \text{ g}^{-1}$  (from  $\text{N}_2$  physisorption). For the experiments in the photoreactor, 100 mg of the sample was pressed into a pellet with a diameter of 1 cm and a thickness of  $\sim 1$  mm.

### 2.3 | UV-Visible Spectroscopy

Spectra were measured at room temperature with a UV-Vis-NIR diffuse reflectance spectrometer (PerkinElmer LAMBDA 365 UV/Vis Spectrophotometer) with a photometric range of 200–1100 nm and an integrating sphere. An identical P25 pellet was remeasured at fixed time intervals. Throughout the measurements, the sample was exposed to ambient air. The equation

$$F(R) = \frac{(1-R)^2}{2R} = \frac{K}{S}$$

with  $R$ : reflectance,  $K$ : absorption coefficient, and  $S$ : scattering coefficient was used to convert diffuse reflectance data  $R$  to Kubelka–Munk function  $F(R)$ , assuming the presence of an infinitely thick P25 pellet.

### 2.4 | Photocatalytic 2-Propanol Oxidation

Experiments were conducted in our high-purity gas-phase photoreactor as described elsewhere [30]. All experiments were conducted at room temperature and under batch reaction conditions. For each experiment, a fresh pellet of the respective sample was used. The pellet was inserted into the photoreactor, and 100  $\mu\text{l}$  of 2-propanol was added dropwise using a microliter pipette. The irradiation window was fixed on top of the reactor, thereby sealing it from the environment. The reactor was flushed with He (99.9999% purity) for 2 h. In previous studies, it has been demonstrated that a residual oxygen concentration of less than 1 ppm can thus be achieved [31]. Afterward, the reactor was filled with He to a pressure of  $\sim 1200$  mbar, upon which the inlet and outlet valves of the reactor were closed. The pellet was then irradiated for 5 h in batch mode with a 200 W Hg/Xe lamp, providing a light intensity at the position of the pellet of  $\sim 200 \text{ mW cm}^{-2}$ . For most experiments, the gas phase in the reactor was entirely sealed off, which means that no gas phase analysis could be performed. To prove the feasibility of 2-propanol oxidation under the given conditions, one selected experiment with a P25 pellet was carried out with gas analysis. The conditions are mostly similar to the procedure described above, but after the 2 h purging step, the reactor was initially filled to  $\sim 1500$  mbar He. Afterwards, gas sampling was performed every 45 min using a Shimadzu GC-2010 TRACERA gas chromatograph, as described elsewhere [30].

To compare the behavior of the aerogel to Ref. [29], its reduction was induced by reaction with methanol in presence of water under continuous flow conditions. After inserting the pellet into the reactor, the reactor volume was purged for 2 h with a flow of  $20 \text{ ml min}^{-1}$  of He (99.9999% purity) previously passed through a stainless-steel saturator filled with 20 Vol-% methanol in water and kept at  $20^\circ\text{C}$ . The absence of  $\text{O}_2$  was confirmed by GC

analysis before irradiation was started. During irradiation, the He flow saturated with methanol/water was maintained.

### 2.5 | Photocharging in Gas-Phase Fixed-Bed Flow Photoreactor

Photocharging of titania aerogel in loose powder form was carried out using a fixed-bed flow photoreactor made of glass. The photoreactor, with an irradiated area of  $4 \text{ cm}^2$  ( $2 \text{ cm} \times 2 \text{ cm}$ ) and a thickness of 0.7 cm, was completely filled with titania aerogel. The aerogel powder was fixed by glass wool plugs at the inlet and the outlet. Two UV-LEDs (365 nm) were located on the opposite side of the reactor at a distance of 1 cm from the reactor. The UV-LEDs utilized in this study have been comprehensively characterized in our previous work [32]. Based on that characterization, the incident photon flux is  $5.7 \mu\text{mol photon s}^{-1}$  and the emission line width is approximately 16 nm. All photocharging experiments were conducted with an LED operating current of 0.65 A. The flow chart of the experimental setup is shown in Figure S1. An Ar stream was first passed through the saturator filled with 20 vol% alcohol-water (100 mL total volume) and subsequently passed through the fixed-bed photoreactor. The Ar flow rate was maintained at  $40 \text{ mL min}^{-1}$ . After purging the reactor for 1 h with alcohol-saturated Ar, the two LEDs positioned on the opposite sides of the reactor were switched on. Photographs of the sample were taken after defined periods of photocharging. A microGC (DynamIQ-S from *qmicro* equipped with a TCD detector and a U column) was used to detect hydrogen.

### 2.6 | Hue Saturation Value (HSV) Analysis

The analysis of the color depths of the samples was performed by HSV analysis using the standard package in Python 3.9. Color was transformed from the RGB scale to the HSV scale, and the hues, i.e., the colors corrected by the saturation and the value (i.e., black components), were compared for the different samples.

## 3 | Results

Figure 1A displays the results of the gas-phase analysis of photocatalytic degradation of 2-propanol on  $\text{TiO}_2$  P25. The degradation reaction, likely caused by photogenerated holes, leads to the formation of increasing amounts of ethane, methane, and CO in the gas phase of the reactor. When simply counting atoms, all these molecules are easily obtained by C–C and/or C–O dissociation steps of the 2-propanol molecule. The formation of these molecules does not require any additional oxygen atoms, so it is not possible to determine whether any oxygen has been removed from the  $\text{TiO}_2$  lattice. At the end of the reaction time, we find 1356 ppm ethane, 856 ppm methane, and 735 ppm CO in the gas phase. Calculating the number of C and H atoms from these values under the assumption that all gases behave ideally, it would result in a hypothetical concentration of  $\sim 1434$  ppm of 2-propanol when calculated from C atoms, which corresponds excellently to the hypothetical 2-propanol concentration of

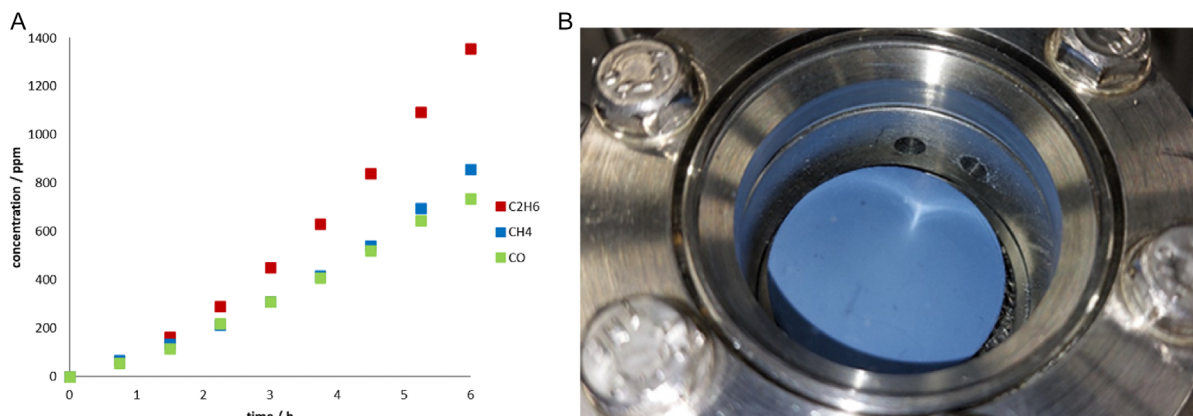


**FIGURE 1** | (A) Gas chromatography of the reaction products obtained from photocatalytic 2-propanol degradation on TiO<sub>2</sub> P25 under batch conditions in pure He; (B) photo of the P25 pellet after the reaction.

1445 ppm estimated from the H atoms. However, the amount of oxygen atoms liberated into the gas phase in the form of 735 ppm CO corresponds to only approximately half of that value. This would even indicate a net addition of oxygen atoms to the surface, rather than a formation of oxygen vacancies.

Mechanistically, surface science experiments have demonstrated Photo-Kolbe reactions involving surface acetates as a source of methyl radical formation, which leads to the formation of ethane (by recombination of two methyl radicals) or methane (by recombination with a hydrogen radical) [33–35]. Indeed, considering our previous studies [22, 25], it is very likely that additional surface products such as acetate or CO<sub>2</sub> have been formed, which requires the participation of additional oxygen atoms compared to the 2-propanol stoichiometry. Under conditions excluding gaseous oxygen, these atoms can only come from another 2-propanol molecule, or from the surface, which may include hydroxyl groups. When acetates decompose in Photo-Kolbe reactions, they should liberate the methyl radical and CO<sub>2</sub> [33–35], but here, only CO is observed, so the oxygen atom needed to form the acetate likely remains in the surface structure. If this oxygen atom resulted from the surface, the net amount of oxygen atoms would be identical after the reaction, but if it resulted from another 2-propanol molecule, the amount of oxygen in the surface would increase rather than decrease during the reaction.

Therefore, the formation of oxygen vacancies is not certain, even when relating our observations to surface science knowledge. This contradicts common assumptions that link the blue color to the formation of Ti<sup>3+</sup> at oxygen vacancies [9]. Computational studies on the possibility of stabilizing “blue” states in titania without introducing oxygen vacancies are currently ongoing. Yet, our preliminary computational results (see description in the Supporting Information, together with Figures S2 and S3) also show that oxygen vacancies are required in the structure to lead to an increased absorbance in the visible range.

As shown in Figure 1B, the P25 pellet was intensely blue colored after the reaction. The pellet was also blue on the reverse side, yet not in its core (Figure S4).

The reactor geometry does not allow UV-visible spectroscopy in situ; however, for one P25 pellet, the absorption of the sample

was measured repeatedly ex situ, whereby the sample was continuously exposed to air. It should be noted that this includes brief initial contact with air before the first spectrum was measured. Figure 2 displays the ex situ UV-vis spectra of a P25 pellet treated identically to the one shown in Figure 1B. Clearly, the band gap absorption below ~400 nm is always unchanged, but the reduced sample shows a broad absorption across almost the entire measurable spectral range. It demonstrates again the success of the reduction of the TiO<sub>2</sub> samples by making them photo-oxidize 2-propanol. Over time, the absorption related to the reduced state decreases but is still noticeable even after 30 h in ambient air, and even on the reverse side of the pellet.

Before starting comparative studies with the different TiO<sub>2</sub> crystal phases, some control experiments were conducted to evaluate possible unexpected influencing factors (Figures S5–S7). First, oxidation processes of native impurities on the different TiO<sub>2</sub> materials might also lead to blue coloring under irradiation, as is demonstrated with a P25 pellet sealed and irradiated in

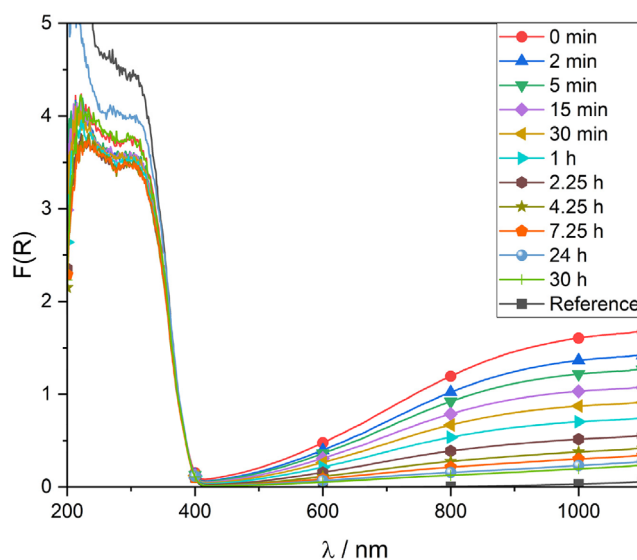


**FIGURE 2** | Ex situ UV-vis spectra of a P25 pellet, reduced by 2-propanol photooxidation for 5 h in the high-purity photoreactor; transfer to spectrometer involved brief exposure to ambient atmosphere; diffuse reflectance data was converted to Kubelka-Munk function  $F(R)$ .

the photoreactor without exposure to 2-propanol. But the effect is less pronounced compared to the color caused by 2-propanol photooxidation (Figure S5). Calcination of P25 before the experiment can partially remove those native impurities, so that a less blue coloring of the sample is observed when irradiated in absence of 2-propanol (Figure S6). The position at which 2-propanol is dropped onto the pellet has no influence, because a homogeneous blue color is obtained, even if 2-propanol is purposefully dropped only on one half of the pellet (Figure S7). It is likely that 2-propanol is readily distributed throughout the reaction atmosphere via the gas phase, so that it also becomes evenly distributed over the surface of P25.

The homogeneous distribution of the color across the exposed macroscopic surface of the pellet, even on the reverse side, yet not in its core, might indicate a certain, yet limited, mobility of color centers throughout the material. Different experiments were conducted to study the migration of color centers in more detail, each with its own benefits and limitations, as will be discussed below. In Figure 3, all the pictures display the state of the sample after 5 h of irradiation while still in the sealed reactor (left), and after removal of the sample from the reactor (right). In the first experiment (Figure 3, top row), half of the pellet was covered in aluminum foil. After removal from the reactor, the covered half was mostly blue, but it cannot be excluded that the light was reflected in tiny gaps between the pellet and the foil. In addition, aluminum foil is a conductor, so if excess charge carriers cause the color, transportation through the foil cannot be excluded. Thus, the cover was exchanged with a non-conducting, inert item that badly transmits light: In the middle row of Figure 3, the results are shown when an alumina crucible was placed face down in the center of the sample. The shape seen when removing the crucible after irradiation is a mostly white ring surrounding a light blue circle. On the other hand, the chipped-off flake on the edge of the pellet displays that the inside of the pellet is clearly white (Figure 3, middle row, right picture). This indicates that the slight blue color below the alumina crucible is rather caused by a residual light transmission through

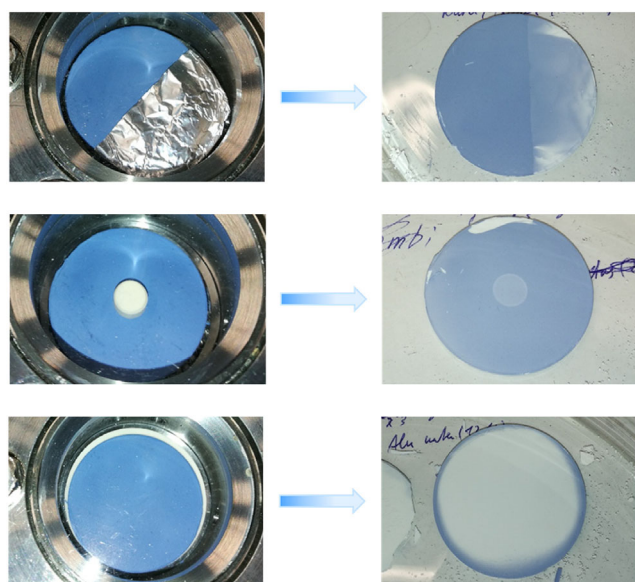


**FIGURE 3** | Tests for the migration of color centers.

the alumina, and that the charges are badly mobile. In a final experiment, a pressed alumina pellet was placed in the reactor first, and then the  $\text{TiO}_2$  pellet was placed on top of it. This should entirely shade the bottom side from any light and any conductor (the metallic reactor bottom). Clearly, the reverse side of the pellet remains white, whereas the edges are slightly blue. Although some light penetration at the edges between the alumina and the titania pellet cannot be excluded, it indicates that the color centers can migrate a certain distance, yet to a limited extent.

The influence of the  $\text{TiO}_2$  polymorph on color evolution and stability is displayed in Figure 4. All samples were identically treated as described in the experimental section. The large surface area, partially amorphous material Hombikat (top row), was mildly blue colored after 15 min and retained this color even after prolonged irradiation for 5 h. The blue color was lost quickly after opening the reactor, and the pellet had turned completely white after 15 min. The pure anatase material was slightly darker blue after the photocatalytic oxidation of 2-propanol, and it also retained the color for an extended period of time but was white again after 18 h. A pure rutile material of similar particle size showed a similar color depth after 5 h of irradiation in the reactor, but it was still slightly blue even after 3 days in ambient atmosphere. P25 (bottom row) was most intensely colored after irradiation, and it retained the color for the longest time frame, with some blue shades remaining even after 4 days in ambient atmosphere (Figure 4). Comparing the results from P25 in Figure 4 with those from Figure S7, it also becomes clear that a longer irradiation time causes a longer color persistence after exposure to ambient atmosphere: Whereas the pellet irradiated for 5 h remained slightly blue for 4 days and more, the pellet irradiated for only 30 min was already mostly white again after 5 h (Figure S7).

All experiments displayed in Figure 4 were conducted with the full spectrum and intensity of the 200 W Hg/Xe lamp. When the UV light intensity was reduced by half, no difference in color intensity after 5 h irradiation or after 30 min in ambient air was noticed (Figure S8). When a filter was additionally used to cut the UV light from the irradiation spectrum, the pellet was only slightly and inhomogenously blue after 5 h of irradiation, and the color was lost quickly (Figure S8). Thus, excitation of electrons across the bandgap is required to induce a blue color,

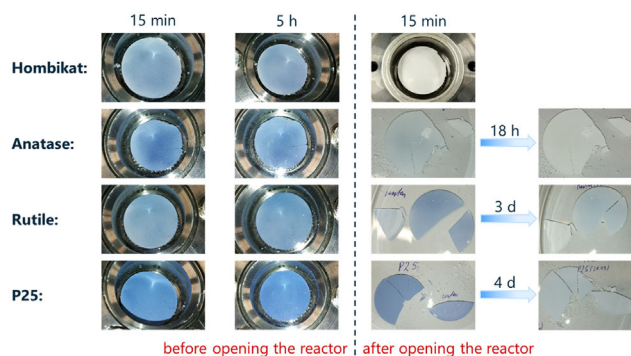


**FIGURE 4** | Color evolution upon irradiation of the different  $\text{TiO}_2$  pellets in presence of 2-propanol, and changes in color after removal of the samples from the reactor and exposure to ambient atmosphere.

which verifies that indeed a photocatalytic step is involved in 2-propanol degradation.

To compare the colors more quantitatively, an HSV analysis of photos of the samples, all taken 15 min after removal from the reactor, was performed (Figure 5). To exclude any influence of other color shades in the picture or of cracks/crumbs on the pellet, the analysis was performed for each sample in a selected  $1 \times 1$  cm area that is as homogeneous as possible in its color distribution (Figure 5, top row). P25 and the rutile sample showed rather similar contributions of dark blue color, whereas only a pale blue, slightly greenish color was detected for the anatase sample. Lastly, blue components were not detected for the Hombikat sample.

The observations with P25 in comparison to the anatase and rutile crystal phases alone led to the question of the behavior of a physical mixture of anatase and rutile. So, a pellet was pressed containing Hombikat in one half, and rutile in the other half. Figure 6 shows that it did not behave like P25, but instead the phases behaved independently in the reaction: Just as observed in Figure 4, Hombikat developed a blue color quickly, whereas it seemed to take longer for rutile. But rutile retained its color upon opening the reactor, whereas Hombikat immediately discolored back to white. It must be noted here that the mixed pellet was unstable and broke when transferred to the reactor.

However, the color distribution indicates that the cracks did not evolve between the two phases, but that the phases were in direct physical contact at several places, despite the cracks. The results indicate that the longer lifetime of the blue state in P25 is not due to the presence of a physical mixture of both phases, but rather due to the presence of interfaces on the nanoscale. This corresponds well to previous observations, where nanoscale contact between anatase and rutile in Au/TiO<sub>2</sub> was found essential for efficient charge separation by electron transfer from rutile to anatase across the interface, which consecutively resulted in high activity in photocatalytic hydrogen evolution [36].

So far, all experiments were performed under exclusion of oxygen. To study the influence of oxygen, a fresh P25 pellet was introduced into the reactor, and 2-propanol was added, but after closing the reactor, the ambient atmosphere was not purged from it. Instead, He was added to reach  $\sim 1200$  mbar as in all other experiments. This should result in an O<sub>2</sub> concentration of  $\sim 16\%$ . The color evolution of this pellet is displayed in Figure 7. Obviously, it is still possible to reduce the TiO<sub>2</sub> pellet, which is explained by the slow transfer of photogenerated electrons over the interface to O<sub>2</sub>, as shown previously [25]. The blue color deepens very slowly at first, but after 2.5 h it is hardly discernible from the color of a pellet reacting with 2-propanol without O<sub>2</sub> (Figure 4). Interestingly, the pressure in the reactor

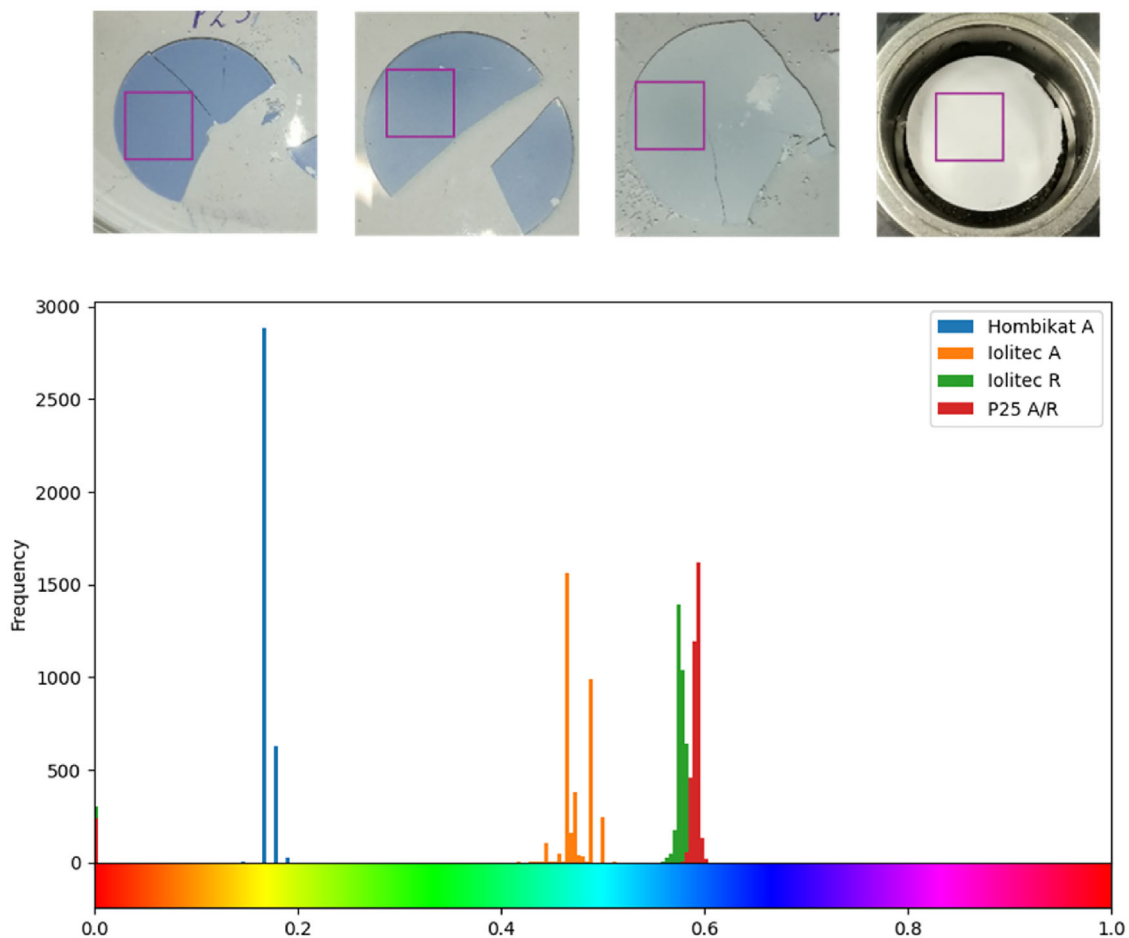


**FIGURE 5** | Top row: Photos of P25 (left), rutile (left center), anatase (right center), and Hombikat (right), 15 min after removal from reactor; a  $1 \times 1$  cm area was selected for each sample (purple box); Bottom: Hue histograms of the areas marked by the purple box on each sample.



**FIGURE 6** | Photodegradation of 2-propanol on a mixed rutile–Hombikat pellet.

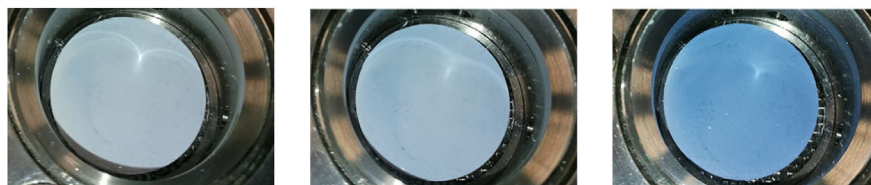


**FIGURE 7** | Color evolution of a P25 pellet in 2-propanol photooxidation in presence of  $O_2$ ; after 20 min (left), after 1 h (center) and after 2.5 h (right). Pressure recording; 1190 mbar at 20 min; 1150 mbar at 1 h, 1130 mbar at 2.5 h.

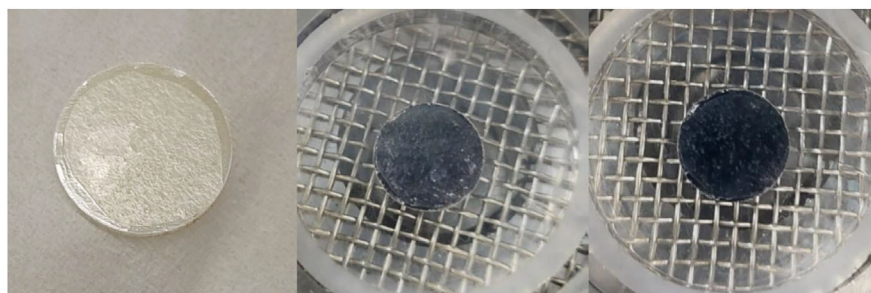
decreased from initially 1200 mbar to eventually 1130 mbar after 2.5 h. This net removal of molecules from the gas phase can be best explained by the formation of strongly bound surface species, such as acetates or carbonates, as observed previously [22]. Since several chemical oxidation steps of 2-propanol are required for the formation of such species, it is likely that they are formed only in the presence of  $O_2$ . Once formed, carbonates might act as hole scavengers, as discussed previously [37], which would increase the amount of excess electrons and possibly cause a deeper blue color after long reaction times (2.5 h, Figure 7).

Having acquired systematic insight into the behavior of the reference materials, an aerogel material is now considered that functioned as a “dark photocatalyst” in a previous work [29]. Since less material was available, only a 1 cm pellet was considered. After pressing (Figure 8), the pellet looks almost transparent to light in the visible spectrum, although the contact edges of the pressed particle agglomerates are still visible. During irradiation in the  $CH_3OH/H_2O/He$  flow, an intense dark blue color is already visible after only 2 min, and after an irradiation of 6 h, the sample appears almost black (Figure 8). Similar to the observations in liquid water, the presence of  $H_2O$  molecules does not hinder the blue coloration of  $TiO_2$ . It appears that consumption of electrons by reduction of protons to  $H_2$  does not occur to a major extent. Since the flow rate in this experiment is  $20\text{ ml min}^{-1}$ , and the detection limit for  $H_2$  of the attached GC is  $>20\text{ ppm}$ ,  $H_2$  formation would only be observed in this experiment if it exceeds  $1\text{ }\mu\text{mol h}^{-1}$ . Likewise, in Ref. [29], noticeable

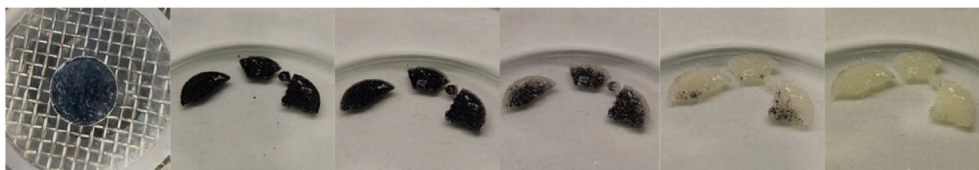
hydrogen evolution was only observed after Pt was deposited on the photocharged aerogel. This is reasonable, given that bare  $TiO_2$  does not feature high catalytic activity for hydrogen evolution.

Figure 9 shows the color stability of the aerogel in contact with air. The blue–black color is very stable for  $\sim 30$  min. Afterwards, discoloration visibly proceeds inhomogeneously. It appears that the separate particle agglomerates within the pellet discolor at different times, with the best accessible ones at the edges of the (broken) pellet discoloring the fastest. Some particle agglomerates at the edge of the aerogel pellet did not lose the black color at all during the observation time of a total of 30 h (Figure S10). In addition, a gradual change of color, e.g., an intermediate blue or gray state, is not detected. Instead, each separate particle agglomerate within the pellet appears either black or colorless. This observation differs significantly from the reference material, which discolored homogeneously across the entire pellet, thereby proceeding through different shades of blue. The exact reasons for the unusual behavior of the aerogel are not known, and future work should study this phenomenon further.

The long time needed for the (almost) complete discoloration of the aerogel is unexpected, given that it is a high-surface-area semi-crystalline anatase material. The nanoparticulate material Hombikat discolored rapidly upon air contact. Possibly the mixed-phase nature of the gel and specific interfaces in the highly interlinked nanoparticulate network of the aerogel lead to a



**FIGURE 8** | Color evolution of the anatase  $TiO_2$  aerogel; fresh pellet (left), after 2 min irradiation in  $CH_3OH/H_2O/He$  flow (center) and after 6 h irradiation in the same gas flow (right).



**FIGURE 9** | Aerogel pellet after opening the reactor, and after air contact for 2 min, 30 min, 1 h 15 min, 2 h, and 3 h (left to right); it must be noted that the displayed pellet is the same as in Figure 8, but it underwent a second reaction cycle in  $\text{CH}_3\text{OH}/\text{H}_2\text{O}/\text{He}$  under batch reaction conditions without intermediate air contact, in which the color hardly changed (Figure S9).

strongly differing behavior. This would be in line with the observations made with P25, where likely the interfaces between anatase and rutile are responsible for its higher color stability. It also highlights the high potential of aerogels, rather than commercial anatase, for charge storage, for example, for the purpose of “dark photocatalysis”: Whereas air contact must be avoided at all costs for commercial anatase materials such as Hombikat, even when they are pressed into pellets, short air contact of aerogel pellets is not critical. Most of the charges trapped in the material remain unaffected in such cases, significantly facilitating the handling of such materials.

For comparison, titania aerogel was also used without pelletization in a smaller gas-phase flow photoreactor to perform photooxidation of 2-propanol. In correspondence with Ref. [29], we refer to this process here as “photocharging”. Photographs of the sample were recorded at specified photocharging times. As shown in Figure 10, even very short irradiation periods, e.g., 1 min, result in noticeable color change of titania aerogel to blue.

Prolonged photocharging leads to more intense coloring of the titania aerogel towards dark blue. However, after 10 min no further additional color change was visually noticeable.

It was also tested whether the type of alcohol had any effect on  $\text{TiO}_2$  coloration. Indeed, different short-chain alcohols (methanol, ethanol, isopropanol) allowed to photocharge the  $\text{TiO}_2$ , and dark blue color was observed in every case (see Figure 11). The color depth was visibly identical in all cases. The highly sensitive microGC of the flow photoreactor allowed the detection of certain amounts of hydrogen during the photocharging process for all the experiments using different alcohols as hole scavengers. Photocharging in the presence of isopropanol produced  $0.24 \mu\text{mol h}^{-1}$  of hydrogen, ethanol produced  $0.35 \mu\text{mol h}^{-1}$ , and methanol generated the highest amount at  $0.52 \mu\text{mol h}^{-1}$ . Indeed, this is below the detection limit of the GC attached to the high-purity photoreactor used for the pellet experiments. Notably, hydrogen evolution ended upon switching off the LEDs, while the dark blue color of the titania aerogel

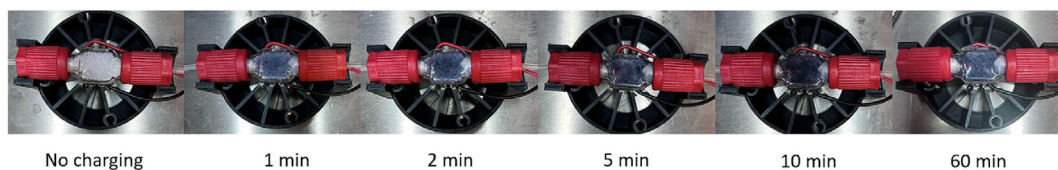


**FIGURE 10** | Photocharging of titania aerogel in the gas-phase. Photographs of the sample taken at different photocharging times. Argon flow rate:  $40 \text{ mL min}^{-1}$ , saturated with 20 vol% methanol–water mixture.

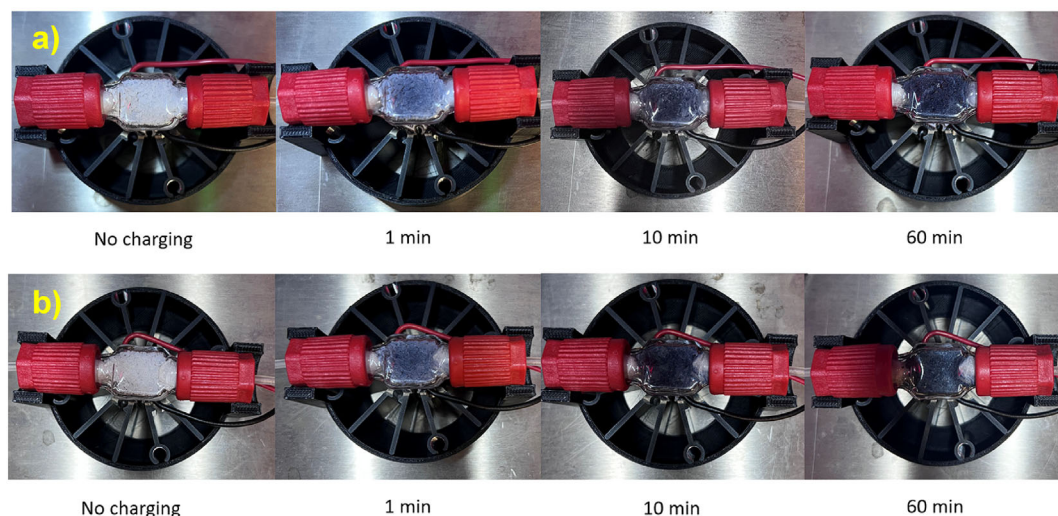


**FIGURE 11** | Photocharging of titania aerogel in gas-phase using (a) ethanol, and (b) isopropanol as hole scavenger. Photographs of the sample were taken at different photocharging times. Argon flow rate:  $40 \text{ mL min}^{-1}$ , saturated with 20 vol% alcohol–water mixture.

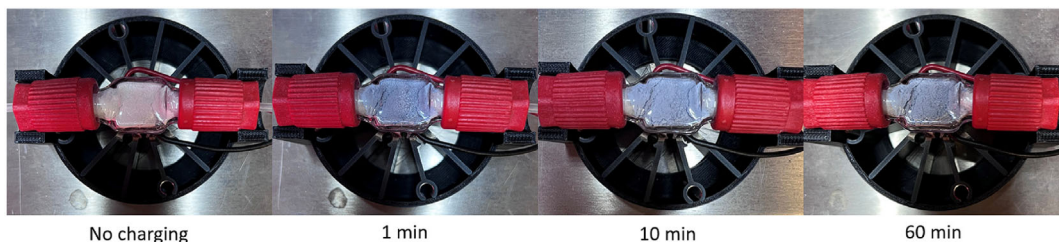


**FIGURE 12** | Photocharging of Hombikat UV100 in the gas phase. Photographs of the sample were taken at different photocharging times. Argon flow rate:  $40 \text{ mL min}^{-1}$ , saturated with 20 vol% methanol–water mixture.

remained, leading to the conclusion that the material was not significantly discharging in the dark.

The measured photocatalytic  $\text{H}_2$  evolution rates show a strong dependence on the molecular properties and thermodynamic oxidation potential of the alcohol sacrificial agents, as previously discussed by Chen et al. [38]. Table S1 summarizes this data. Methanol, which holds three  $\alpha$ -H atoms and the lowest standard oxidation potential (0.016 V vs. NHE), facilitates the most rapid surface oxidation. Remarkably, this reactivity trend aligns seamlessly with the ultrafast hole-scavenging dynamics reported by Tamaki et al. [39], where trapped hole lifetimes in  $\text{TiO}_2$  were measured to be 300, 1000, and 3000 ps for methanol, ethanol, and isopropanol, respectively. The combination of these favourable thermodynamic and kinetic properties directly translates to the higher  $\text{H}_2$  production rates observed for methanol in our system.

Gas-phase photocharging of Hombikat UV100 powder under continuous flow conditions was tested for comparison. Figure 12 shows photographs of a sample at different photocharging times. The color of Hombikat changes to light blue upon illumination and does not change visually even with extended photocharging time, different from the titania aerogel, which turns to a dark blue. Moreover, the hydrogen production rate of Hombikat using methanol as a hole scavenger was  $0.72 \mu\text{mol h}^{-1}$ , which is about 50% more than observed for the titania aerogel.

Both photocharged titania powder materials discharged immediately upon opening the reactor and exposing the material to air. This behavior differs from the pelleted samples, which retain their color for longer time. This observation gives evidence that the slower discharge in pellets results from a limited diffusion of oxygen into the pellet. This is another relevant piece of information for researchers aiming to apply blue titania for various applications.

## 4 | Conclusions

All  $\text{TiO}_2$  polymorphs can be colored blue when they photooxidize 2-propanol in the absence of oxygen. Rutile can stabilize the blue state better than anatase, so that the color is retained for a longer time (>3 days). P25, being a mixture of anatase and rutile, reaches the deepest coloration and retains the color the longest time. Likely, the behavior of P25 cannot be explained by functioning as a simple physical mixture of anatase and rutile,

because in a mixed Hombikat:rutile pellet, both phases reacted independently from one another. The charge carriers causing the blue color might be slightly mobile, but only to a limited extent. Even in the presence of oxygen, blue coloration of  $\text{TiO}_2$  is still observed, but it takes more time to reach a deep color. The pressure in the reactor drops slightly, which possibly indicates the formation of highly oxidized surface species such as acetates or carbonates. They may function as hole traps, thereby allowing the storage of excess electrons in  $\text{TiO}_2$  at later time periods. Aerogels rapidly reached an almost black color during irradiation in alcohol/ $\text{H}_2\text{O}$ /He flow. Despite their semi-crystalline structure and high surface area, the color of the aerogel pellet was retained for hours under exposure to air. The aerogels discolored inhomogeneously and “agglomerate by agglomerate”, whereby no intermediate states between black and colorless were observed. Some particles did not discolor at all during the observation time of 30 h. In contrast, the aerogel immediately discolored when it was photocharged as powder, giving evidence that limited oxygen diffusion into the pellets causes the long-lasting coloring.

The results can provide guidance to researchers aiming to store charge carriers in  $\text{TiO}_2$ , which may be more successful with rutile than anatase, or even more so with mixed-phase  $\text{TiO}_2$ , such as P25. High surface area seems beneficial to reach the blue color quickly, but it is detrimental in retaining the charge carriers in the material, unless the accessibility of the particles to oxygen is limited, particularly in aerogel pellets. In addition, complete oxygen exclusion may not be required to reach a blue color through photodegradation of alcohols. Our ongoing and future work is aimed at providing a more detailed understanding of potential different features causing a blue state (e.g., oxygen vacancies, excess electrons, foreign atoms, etc.) and on providing a mechanistic understanding of the role of the surface species formed on  $\text{TiO}_2$  from 2-propanol oxidation on color evolution and color retention.

## Acknowledgments

Part of the work was funded by the German Ministry of Education and Research (BMBF) in the scope of the project *PRODIGY*, FKZ 033RC024A. Part of the work was funded by the German Research Foundation (DFG), within the scope of the Priority Programm 2370 “Nitroconversion”, within the project “Ammonia on Demand” (project no. 501591928). Scientific exchange with Roland Marschall, University of Bayreuth, and Barbara Milow, German Aerospace Center, is gratefully acknowledged.

Open Access funding enabled and organized by Projekt DEAL.

## Funding

This study was supported by Bundesministerium für Bildung und Forschung (033RC024A), Deutsche Forschungsgemeinschaft (501591928).

## Conflicts of Interest

The authors declare no conflicts of interest.

## Data Availability Statement

The data that support the findings of this study are available from the corresponding author upon reasonable request.

## References

1. C. W. Carstens, "XVI. Über Das Auftreten Des Titans in Den Titanhaltigen Schlacken (mit Besonderer Berücksichtigung Des Titanmonoxyds)," *Zeitschrift für Kristallographie - Crystalline Materials* 67 (1928): 260.
2. P. Ehrlich, "Phasenverhältnisse Und Magnetisches Verhalten Im System Titan/Sauerstoff," *Zeitschrift für Elektrochemie und angewandte physikalische Chemie* 45 (1939): 362.
3. P. Ehrlich, "Lösungen Von Sauerstoff in Metallischem Titan," *Zeitschrift Für Anorganische Und Allgemeine Chemie* 247 (1941): 53.
4. S. Zerfoss, R. G. Stokes, and C. H. Moore Jr, "Notes on the Properties of Synthetic Rutile Single Crystals," *The Journal of Chemical Physics* 16 (1948): 1166.
5. G. Johnson and W. A. Weyl, "Influence of Minor Additions on Color and Electrical Properties of Rutile," *Journal of the American Ceramic Society* 32 (1949): 398.
6. C. Renz, "Lichtreaktionen der Oxyde Des Titans, Cers Und der Erdsäuren," *Helvetica Chimica Acta* 4 (1921): 961.
7. A. E. Jacobsen, "Titanium Dioxide Pigments: Correlation between Photochemical Reactivity and Chalking," *Industrial & Engineering Chemistry* 41 (1949): 523.
8. W. A. Weyl and T. Förland, "Photochemistry of Rutile," *Industrial & Engineering Chemistry* 42 (1950): 257.
9. U. Diebold, "The Surface Science of Titanium Dioxide," *Surface Science Reports* 48 (2003): 53.
10. X. Chen, L. Liu, P. Y. Yu, and S. S. Mao, "Increasing Solar Absorption for Photocatalysis with Black Hydrogenated Titanium Dioxide Nanocrystals," *Science* 331 (2011): 746.
11. F. Zuo, L. Wang, T. Wu, Z. Zhang, D. Borchardt, and P. Feng, "Self-Doped Ti<sup>3+</sup> Enhanced Photocatalyst for Hydrogen Production Under Visible Light," *Journal of the American Chemical Society* 132 (2010): 11856.
12. Z. Hao, Q. Chen, W. Dai, et al., "Oxygen-Deficient Blue TiO<sub>2</sub> for Ultrastable and Fast Lithium Storage," *Advanced Energy Materials* 10 (2020): 1903107.
13. J. Qiu, S. Li, E. Gray, et al., "Hydrogenation Synthesis of Blue TiO<sub>2</sub> for High-Performance Lithium-Ion Batteries," *The Journal of Physical Chemistry C* 118 (2014): 8824.
14. J. Zheng, G. Ji, P. Zhang, et al., "Facile Aluminum Reduction Synthesis of Blue TiO<sub>2</sub> with Oxygen Deficiency for Lithium-Ion Batteries," *Chemistry – A European Journal* 21 (2015): 18309.
15. H. Tan, Z. Zhao, M. Niu, et al., "A Facile and Versatile Method for Preparation of Colored TiO<sub>2</sub> with Enhanced Solar-Driven Photocatalytic Activity," *Nanoscale* 6 (2014): 10216.
16. S. Oh, J.-H. Kim, H. M. Hwang, et al., "Band Restructuring of Ordered/Disordered Blue TiO<sub>2</sub> for Visible Light Photocatalysis," *Journal of Materials Chemistry A* 9 (2021): 4822.
17. S. Wu, M. Y. Manuputty, Y. Sheng, et al., "Flame Synthesized Blue TiO<sub>2-x</sub> with Tunable Oxygen Vacancies from Surface to Grain Boundary to Bulk," *Small Methods* 5 (2021): 2000928.
18. M. S. Hamdy, R. Amrollahi, and G. Mul, "Surface Ti<sup>3+</sup>-Containing (blue) Titania: A Unique Photocatalyst with High Activity and Selectivity in Visible Light-Stimulated Selective Oxidation," *ACS Catalysis* 2 (2012): 2641.
19. Y. J. Lee, L. K. Putri, B.-J. Ng, L.-L. Tan, T. Y. Wu, and S.-P. Chai, "Blue TiO<sub>2</sub> with Tunable Oxygen-Vacancy Defects for Enhanced Photocatalytic Diesel Oil Degradation," *Applied Surface Science* 611 (2023): 155716.
20. G. Zhu, Y. Shan, T. Lin, et al., "Hydrogenated Blue Titania with High Solar Absorption and Greatly Improved Photocatalysis," *Nanoscale* 8 (2016): 4705.
21. Y. Liu, L. Tian, X. Tan, X. Li, and X. Chen, "Synthesis, Properties, and Applications of Black Titanium Dioxide Nanomaterials," *Science Bulletin* 62 (2017): 431.
22. M. Lang, M. Klahn, and J. Strunk, "Supported Titanium Oxide Species as Photocatalysts in 2-Propanol Oxidation: Linking Selectivity to Structural and Electronic Properties," *Applied Surface Science* 611 (2023): 155623.
23. E. L. Quah, J. N. Wilson, and H. Idriss, "Photoreaction of the Rutile TiO<sub>2</sub>(011) Single-Crystal Surface: Reaction with Acetic Acid," *Langmuir* 26 (2010): 6411.
24. P. M. Jayaweera, E. L. Quah, and H. Idriss, "Photoreaction of Ethanol on TiO<sub>2</sub>(110) Single-Crystal Surface," *The Journal of Physical Chemistry C* 111 (2007): 1764.
25. A. Lükken, M. Muhler, and J. Strunk, "On the Role of Gold Nanoparticles in the Selective Photooxidation of 2-Propanol over Au/TiO<sub>2</sub>," *Physical Chemistry Chemical Physics* 17 (2015): 10391.
26. N. Siemer, A. Lükken, M. Zalibera, et al., "Atomic-Scale Explanation of O<sub>2</sub> Activation at the Au-TiO<sub>2</sub> Interface," *Journal of the American Chemical Society* 140 (2018): 18082.
27. D. Bahnemann, A. Henglein, J. Lilie, and L. Spanhel, "Flash Photolysis Observation of the Absorption Spectra of Trapped Positive Holes and Electrons in Colloidal Titanium Dioxide," *The Journal of Physical Chemistry* 88 (1984): 709.
28. V. W.-h. Lau, D. Klose, H. Kasap, et al., "Dark Photocatalysis: Storage of Solar Energy in Carbon Nitride for Time-Delayed Hydrogen Generation," *Angewandte Chemie International Edition* 56 (2017): 510.
29. A. Rose, A. Hofmann, P. Voepel, B. Milow, and R. Marschall, "Photocatalytic Activity and Electron Storage Capability of TiO<sub>2</sub> Aerogels with an Adjustable Surface Area," *ACS Applied Energy Materials* 5 (2022): 14966.
30. N. G. Moustakas, M. Klahn, B. T. Mei, et al., "A High-Purity Gas-solid Photoreactor for Reliable and Reproducible Photocatalytic CO<sub>2</sub> Reduction Measurements," *HardwareX* 15 (2023): e00448.
31. M. Dilla, A. Jakubowski, S. Ristig, J. Strunk, and R. Schlögl, "The Fate of O<sub>2</sub> in Photocatalytic CO<sub>2</sub> Reduction on TiO<sub>2</sub> Under Conditions of Highest Purity," *Physical Chemistry Chemical Physics* 21 (2019): 15949.
32. A. Valaei, A. Hofmann, A. Rose, et al., "Efficient Light-Driven Charge Storage in Titania Aerogels: From Photochemical Batch Studies to Capillary Flow Reactors," *Chemical Engineering Journal* 524 (2025): 168924.
33. J. N. Wilson and H. Idriss, "Structure Sensitivity and Photocatalytic Reactions of Semiconductors. Effect of the Last Layer Atomic Arrangement," *Journal of the American Chemical Society* 124 (2002): 11284.
34. X. Fu, X. Wang, D. Y. C. Leung, Q. Gu, S. Chen, and H. Huang, "Photocatalytic Reforming of C<sub>3</sub>-Polyols for H<sub>2</sub> Production: Part (I). Role of Their OH Groups," *Applied Catalysis B: Environmental* 106 (2011): 681.

35. D. S. Muggli, S. A. Keyser, and J. L. Falconer, "Photocatalytic Decomposition of Acetic Acid on TiO<sub>2</sub>," *Catalysis Letters* 55 (1998): 129.
36. V. Jovic, K. E. Smith, H. Idriss, and G. I. N. Waterhouse, "Heterojunction Synergies in Titania-Supported Gold Photocatalysts: Implications for Solar Hydrogen Production," *ChemSusChem* 8 (2015): 2551.
37. R. Marschall, L. Schumacher, and J. Strunk, "Shedding Light on Common Misinterpretations in Photocatalyst Characterization," *Advanced Energy Materials* 16 (2025): 2501192.
38. W.-T. Chen, A. Chan, Z. H. N. Al-Azri, et al., "Effect of TiO<sub>2</sub> Polymorph and Alcohol Sacrificial Agent on the Activity of Au/TiO<sub>2</sub> Photocatalysts for H<sub>2</sub> Production in Alcohol-water Mixtures," *Journal of Catalysis* 329 (2015): 499.
39. Y. Tamaki, A. Furube, M. Murai, K. Hara, R. Katoh, and M. Tachiya, "Direct Observation of Reactive Trapped Holes in TiO<sub>2</sub> Undergoing Photocatalytic Oxidation of Adsorbed Alcohols: Evaluation of the Reaction Rates and Yields," *Journal of the American Chemical Society* 128 (2006): 416.

### Supporting Information

Additional supporting information can be found online in the Supporting Information section.